MODELLING OF INTERNAL TRANSPORT BARRIER FORMATION ON TUMAN-3M TOKAMAK

V. Rozhansky, L. Popov* and S. Voskoboynikov

St.Petersburg State Technical University, 195251 St.Petersburg, Russia

**Ioffe Physico-Technical Institute, 195252 St.Petersburg, Russia*

1. Introduction

Transport code is employed for the Tuman-3M tokamak accounting for the reduction of transport coefficients due to the enhanced shear of the $\vec{E}\times\vec{B}$ drift. The evolution of radial electric field is addressed consistently with equations for density, electron and ion temperatures, toroidal current. A novel mechanism for the generation of radial electric field is incorporated into the code. The key element of this mechanism is the radial current, which is caused by the radial particles motion in the toroidal electric field. It is well-known that in the banana regime the toroidal electric field results in the ambipolar Ware drift of the charged particles. However, when the collisionality parameter ν_i^* is of the order of unity (this situation is typical for many modern tokamaks), the Ware drifts of ions and electrons are not automatically equal to each other. In the situation when $\nu_e^* < 1$ and $\nu_i^* > 1$ the ion Ware drift is suppressed, so that the radial current is generated. This current is to be balanced by the radial current associated with the neoclassical parallel viscosity of ions, so that the net radial current remains zero. This effect results in the additional (with respect to the neoclassical one) radial electric field, and, thus, in the creation of the additional shear of the poloidal rotation.

It is demonstrated that for the Tuman-3 parameters this effect can be responsible for the additional suppression of the transport coefficients and for rise of the edge barrier width. In some regimes of Tuman-3M with large plasma current the internal barrier can be formed, due to the additional shear of the poloidal rotation, as was observed experimentally.

2. Model

The following set of transport equations has been solved:

$$\frac{\partial n}{\partial t} - \frac{1}{r}\frac{\partial}{\partial r}[r(D(\omega_s)\frac{\partial n}{\partial r} - V(\omega_s)n] = S\,, \qquad (1)$$

$$\frac{3}{2}n(\frac{\partial T_{e,i}}{\partial t} + \frac{\vec{\Gamma}}{n}\nabla T_{e,i}) + nT_{e,i}\nabla\cdot\frac{\vec{\Gamma}}{n} - \frac{1}{r}\frac{\partial}{\partial r}[r(\frac{3}{2}n\chi_{e,i}(\omega_s)\frac{\partial T_{e,i}}{\partial r}] = Q_{e,i}\,, \qquad (2)$$

$$\frac{\partial B_\vartheta}{\partial t} = \frac{\partial}{\partial r}[\frac{c^2}{4\pi\sigma_\parallel r}\frac{\partial}{\partial r}(rB_\vartheta)]\,. \qquad (3)$$

Here the transport coefficients are supposed to be dependent on the shear of the $\vec{E}\times\vec{B}$ drift

$$\omega_s = \frac{RB_\vartheta}{B}\left|\frac{\partial(E_r / B_\vartheta R)}{\partial r}\right| = \frac{RB_\vartheta}{B}\left|\frac{\partial[(v_\vartheta - u_{pi})B / B_\vartheta R)]}{\partial r}\right|, \qquad (4)$$

where the poloidal velocity $v_\vartheta = E_r / B + u_{pi}$ with u_{pi} being the ion diamagnetic drift velocity. In the Ohmic regime the toroidal rotation is damped by the anomalous viscosity [1-2]. Here $\sigma_\|$ is the parallel neoclassical conductivity. The equation for the radial electric field is

$$\sigma_\perp(E_r - E_r^{NEO}) - \frac{cE_\|}{B_\vartheta}\sqrt{\varepsilon}[\frac{1}{(1+\nu_i^*\varepsilon^{3/2})(1+\nu_i^{*1/3}+\nu_i^*)} - \frac{1}{(1+\nu_i^*\varepsilon^{3/2})(1+\nu_i^{*1/3}+\nu_i^*)}] = 0 \qquad (5)$$

where $\sigma_\perp = \sigma_\perp^b\sigma_\perp^p / (\sigma_\perp^b + \sigma_\perp^p)$ is the perpendicular conductivity, and the conductivities $\sigma_{\perp b}$, $\sigma_{\perp p}$ are calculated in [1,2] for the banana and plateau regimes accordingly

$$\sigma_\perp^b = \frac{n\sqrt{\varepsilon}m_i\nu_i}{B_\vartheta^2}; \quad \sigma_\perp^p = \frac{\sqrt{\pi/2}n\varepsilon^2\sqrt{m_iT_i}}{B_\vartheta Br}. \qquad (6)$$

The neoclassical electric field is given by

$$E_r^{(NEO)} = \frac{T_i}{e}[\frac{\partial \ln n}{\partial r} + (1-k)\frac{\partial \ln T_i}{\partial r}], \qquad (7)$$

where k is the numerical coefficient depending on collisionality. The first term in Eq. (5) describes the magnetic pumping, and in the absence of the second term the neoclassical electric field is formed in the stationary case. Analysis of more complicated equation for radial electric field [3], where the radial transport of poloidal rotation and time-dependent terms were taken into account, demonstrated that radial electric field is close to the neoclassical value provided the last term in Eq. (5) is neglected. However, the second term in Eq. (5) can change significantly the neoclassical value.

The following transport coefficients were chosen. The diffusion coefficient is $D=D_0f(r)$ ($f(r=0)=1$) and the convective velocity $V=-(D_0/a)\psi(r)$ is negative, where a is the LCFS radius. The heat conductivities are $\chi_e=2D$, $\chi_i=D$. The dependence of D_0 on the parameter ω_s is shown in Fig. 1. The radial dependencies of coefficients D and V were chosen to model the experimentally observed density and temperatures profiles before the transition [4]. The source S in Eq. (1) was measured in the experiments both in L and H regimes, these profiles were used for calculations.

3. Results of the simulation

Scenario of the evolution crucially depends on the parameter ω_s. In the case modelled in [4], where electric field was close to the neoclassical value, ω_{s1} was taken to be 0.25 $10^5 s^{-1}$. The maximal shear of **E**x**B** drift corresponds to r=a, and when the chosen value of ω_{s1} has been reached, the L-H transition started. The typical scenario is shown in Figs. 2-3. The edge transport barrier is formed in the narrow region of 1-2cm near LCFS. However, in the experiments [4] the features of VH regime were observed - the reduction of the transport coefficients in the core was registered. Moreover, in the regime with large plasma current [5] the internal transport barrier has been formed.

Calculation of plasma parameters evolution before the transition with accounting of the second term in Eq. (5) is shown in Figs. 4-5. The contribution from additional radial current caused by toroidal electric field (second and third terms in Eq. (5)) results in the strong variation of radial electric field with respect to the neoclassical value, see Figs. 4-5. Furthermore, additional shear of radial electric field arises in the core for r>15cm. The shear of electric field after the transition is shown in Fig. 6 (ω_{s1}=0.45 $10^5 s^{-1}$). It consists of two parts - the strong shear at 1-2 cm from LCFS and a pedestal associated with the new mechanism. This additional shear is sufficient to cause further reduction of the transport coefficients in the internal regions, so that the width of the transport barrier becomes larger, more than 4cm, see Fig. 7. The boundary value of ω_{s1} here can be lower than at the edge, so that one can anticipate further rise of the barrier width with respect to the present model. Moreover, for regimes with larger plasma current [5] the shear of the $\vec{E} \times \vec{B}$ drift in the core can exceed the shear at LCFS. As a result, the internal transport barrier can be formed before the L-H transition occurs. Such situation was apparently observed on Tuman-3M [5].

Acknowledgments

The work was supported by the RFFI grant N 96-02-16919.

References

[1] Rozhansky V., Tendler M.: Phys. Fluids **B4** 1877 (1992)

[2] Rozhansky V., Tendler M: *in* Reviews of Plasma Phys. Ed. by B.B. Kadomtsev, Consultants Bureau, N.Y.-London, **19** 147 (1996)

[3] Rozhansky V., Voskoboynikov S., Tendler M.: *in* Controlled Fusion & Plasma Phys. (*Proc.24th EPS Conf.*, Berchtesgaden 1997) **21A** Part 2 697 (1997)

[4] Andrejko M.V. et al.: Plasma Phys. Contr. Fus. Res. 1992 (*Proc. 14 Int. Conf. Plasma Phys. Contr. Fus.*, Wurzburg 1992) **1** 485 (1993)

[5] Andrejko M.V. et al.: *in* Controlled Fusion & Plasma Phys. (*Proc.24th EPS Conf.* Berchtesgaden 1997) **21A** Part 2 693 (1997)

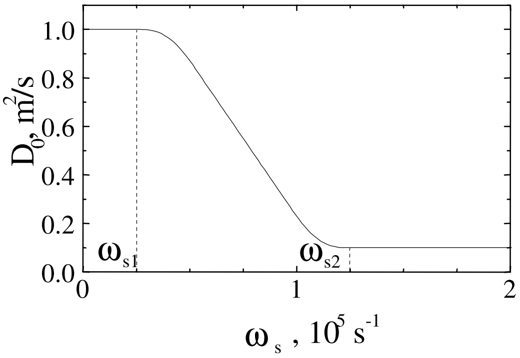

Fig. 1. *The dependence of D_0 on poloidal drift shear.*

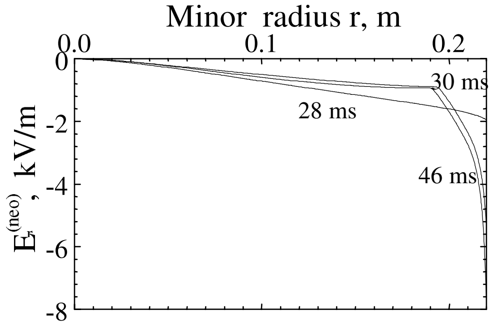

Fig. 2. *Neoclassical electric field.*

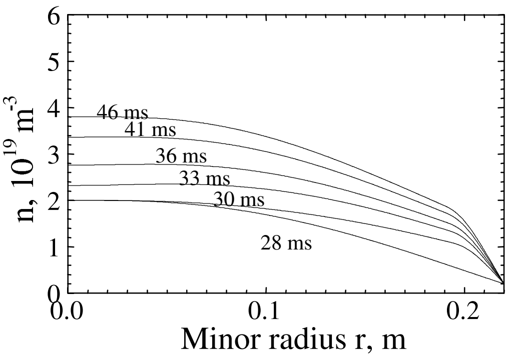

Fig. 3. *Density evolution, calculations.*

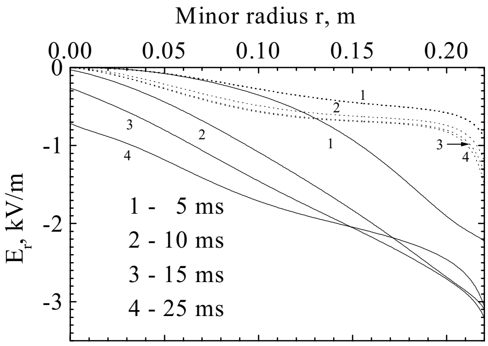

Fig. 4. *Electric field before the transition.*

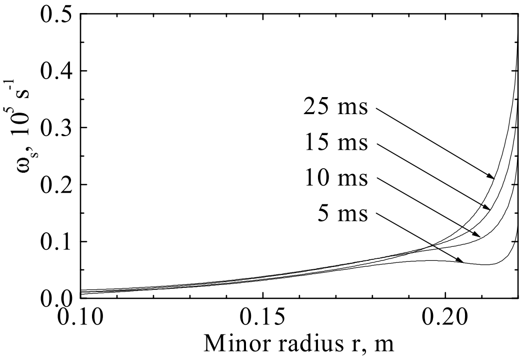

Fig. 5. *Shear of $\vec{E} \times \vec{B}$ drift before the transition*

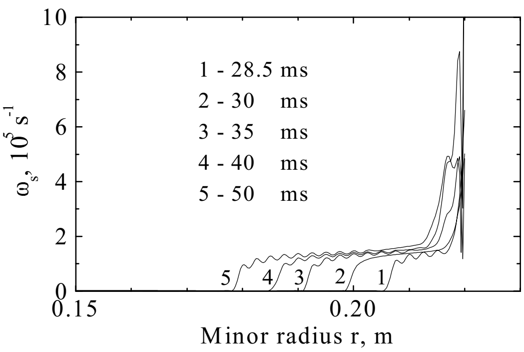

Fig. 6. *Shear of $\vec{E} \times \vec{B}$ drift after the transition*

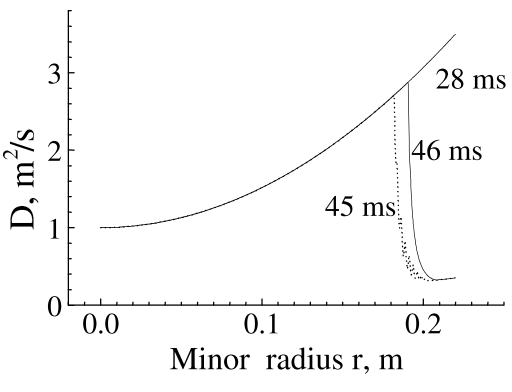

Fig. 7. *Reduction of diffusion coefficient, solid line - neoclassical electric field, dotted line-electric field calculated from Eq.(5).*